Catalytic RNA Reactions of Yeast tRNA^{Phe} Fragments†

Hung-Yin Deng and John Termini*

Department of Molecular Biochemistry, Beckman Research Institute of the City of Hope, 1450 East Duarte Road, Duarte, California 91010

Received March 6, 1992; Revised Manuscript Received June 25, 1992

ABSTRACT: We describe 12 new catalytic RNA reactions which are *intermolecular* variants of the well-known *intramolecular* Pb^{2+}-promoted hydrolysis of yeast tRNA^{Phe}. Fragments derived from the native yeast tRNA^{Phe} which possess the T stem–loop can function as catalysts for the site-specific hydrolysis at p18 of D stem–loop-containing fragments. An initial report described the catalytic cleavage of an unmodified T7 transcript corresponding to the 5′ half of tRNA^{Phe} by a 3′ half-molecule derived from the native tRNA. [Sampson, J. R., Sullivan, F. X., Behlen, L. S., DiRenzo, A. B., & Uhlenbeck, O. C. (1987) *Cold Spring Harbor Symp. Quant. Biol. 52,* 267–275]. We have investigated the trans reaction further by creating a family of substrate and catalyst RNA molecules by dissection of the native tRNA^{Phe} using a combination of chemical and enzymatic methods. A search for cleavage activity in trans was conducted using a combinatorial approach with the available T and D stem–loop-containing fragments. Twelve combinations were found to be catalytic, and initial rates, k_{cat}'s, and K_m's are reported for each. The k_{cat}'s for the reactions differ by ~20-fold, whereas K_m's vary by only ~2-fold. Differences in some of the cleavage rates argue that tertiary interactions present in the intact molecule can be reconstituted in the fragment combinations. Secondary structural features remote from the cleavage site can also affect the apparent cleavage rates. A minimum catalytic complex consisting of a substrate fragment corresponding to nucleotides 1–24 of the native molecule and a catalytic RNA corresponding to 46–76 is identified. This complex is of interest since the transition state for cleavage involves only three helices, with no elements of the anticodon required for cleavage. This is reminiscent of the proposed secondary structure of the hammerhead catalytic RNA cleavage motif.

The reaction of yeast tRNA^{Phe} with Pb^{2+} at pH 7.0 was the first well-characterized example of a metal-promoted site-specific cleavage reaction involving RNA (Werner et al., 1976). X-ray structures (3.5-Å resolution) of tRNA^{Phe} in the presence of lead ion at pH 5.5 and at pH 7.4 allowed for the structure determination of the tRNA^{Phe} reaction complex before and after cleavage. Thus it is the only site-specific metal-promoted cleavage reaction of RNA for which detailed structural knowledge is available (Brown et al., 1983, 1985). Cleavage occurs almost exclusively at the phosphodiester linkage between D_{17}–G_{18}, (p18), resulting in the formation of a 2′,3′-cyclic phosphate at D_{17}. Although the nonenzymatic hydrolysis of RNA by metal ions had been the subject of previous investigations (Dimroth & Witzel, 1959; Butzow & Eichorn, 1965, 1971; Farkas, 1968), the selective nature of the cleavage reaction of yeast tRNA^{Phe} with lead and other metals was unique. The discovery of catalytic RNA or ribozymes (Cech, 1987; Altman, 1989) placed this seemingly anomalous reaction into a broader mechanistic context. The exhaustive structural information obtained by both crystallographic (Kim et al., 1974; Robertus et al., 1974) and NMR solution studies (Johnson & Redfield, 1979; Reid, 1981) of the yeast tRNA^{Phe} make it an obvious candidate for structure–function studies of a catalytic RNA reaction (Sampson et al., 1987; Behlen et al., 1990). It seems likely that some of the structural motifs observed for tRNA^{Phe} could be shared with other catalytic RNAs.

The self-cleavage reaction of tRNA^{Phe} by Pb^{2+} ion has been examined using unmodified T7 RNA polymerase transcripts of the same sequence as that of the native molecule (Behlen et al., 1990). This transcript was found to cleave at a 2-fold slower rate than the native tRNA, although the cleavage site was identical. The effects of base changes on the Pb^{2+} cleavage reaction were studied extensively in the tRNA^{Phe} transcript. Mutations which disrupted the T- and D-loop interactions impaired the cleavage reaction. Some mutants at U_{59} or C_{60} either abolished or severely impaired cleavage. The lead ion is tightly coordinated to these two residues in the native molecule and is one of three that was found in the crystal structure, the other two occupying the variable and anticodon loops (Brown et al., 1985). The T-loop-bound lead is believed to be responsible for the site-specific cleavage reaction at D_{17}, since it is in close contact to the D-loop as a result of tertiary interactions. This region between T- and D-loops defines a preferred site for metal ions, and Mn^{2+}, Mg^{2+}, and Sm^{2+} have been demonstrated by crystallography to occupy this "variable pocket", although with altered geometries (Jack et al., 1977).

The extent to which the self-cleavage reaction of tRNA^{Phe} could be made to occur in an intermolecular, catalytic fashion and thus serve as a model for certain classes of catalytic RNAs was explored in the present studies. An initial report described the catalytic hydrolysis of a tRNA^{Phe} transcript corresponding to the 5′ half-molecule (nucleotides 1–35) by a 3′ half (nucleotides 34–74) ribozyme molecule derived by partial enzymatic digestion of native tRNA^{Phe} (Sampson et al., 1987). That reaction was described as being 5-fold slower than a hammerhead RNA reaction, yet the end products were the same (2′,3′-cyclic phosphate), suggesting a related mechanism.

We wanted to determine whether a minimum catalytic cleavage complex could be found and thus define the essential features required for intermolecular cleavage. The lead-promoted cleavage of the yeast tRNA^{Phe} could be an adventitious property of the entire molecule or a reaction

† Supported in part by grants from the NIH (2S07RR05841) and NCI (CA33572) and the Beckman Foundation.

* Author to whom correspondence should be addressed.

0006-2960/92/0431-10518$03.00/0

defined by only a few interactions reflecting a more general cleavage motif. Our experimental approach was to dissect the T- and D-loop-containing half-molecules into smaller fragments using the RNAse H method and then to characterize all the intermolecular cleavage reactions that resulted upon combining these various fragments in the presence of lead ions. This approach enabled us to define a minimum catalytic complex consisting of T- and D-loop-containing fragments and allowed us to evaluate the effects of tertiary interactions and secondary structural features on the reaction rate.

MATERIALS AND METHODS

Phenylalanine-specific tRNA from yeast was purchased from Boehringer Mannheim Biochemicals and used without further purification. RNAse T1 (molecular biology grade), Tris base, and DTT were also obtained from this supplier. T4 polynucleotide kinase was purchased from New England Biolabs. RNAse Phy M was obtained from Pharmacia LKB. Recombinant ribonuclease H from *Escherichia coli* was obtained from United States Biochemical. Aniline (99.5%) was purchased from Aldrich Chemical Co. and was used without further purification. Spermine, spermidine, and putrescine were from Sigma. HPLC grade triethylamine was purchased from Fischer Scientific. HPLC grade acetonitrile was from Burdick and Jackson. Mono Q HR 5/5 strong anion-exchange column and PepRPC HR 5/5 C_2/C_{18} reverse-phase columns were from Pharmacia.

Half-Molecules from Yeast tRNA^{Phe}. The removal of the wybutine base at position 37 and the subsequent chain scission of tRNA^{Phe}–Y to create 5′ and 3′ half-molecules were carried out as described (Thiebe & Zachau, 1971) with the following modifications. tRNA^{Phe} (1 mg) was resuspended in 1 mL of water and dialyzed overnight against 2 L of water. The pH of the dialysate was then adjusted to 2.7 via the addition of HCl, and the sample was incubated for 3 h at room temperature in order to remove the Y base. The tRNA^{Phe}–Y was then EtOH[1] precipitated, resuspended in 300 μL of 0.45 M aniline/HCl (pH 4.5), and incubated for 5 h in the dark at room temperature. The resultant half-molecules were precipitated by EtOH and resuspended in 500 μL of 50 mM TEAA (pH 6.5). Fragments 1–36 and 38–76 were isolated using a Pep RPC HR 5/5 C_2/C_{18} reverse-phase column on a Pharmacia FPLC instrument, using a gradient of 9–15% acetonitrile in 50 mM TEAA (pH 6.5) over 60 min. Fragments 1–36 and 38–76 were eluted at 9 and 12% acetonitrile, respectively. Half-molecules were concentrated by lyophilization, EtOH precipitated, and stored at −20 °C.

Cleavage of Yeast tRNA^{Phe} at m^{7}G$_{46}$. The procedure for chain scission at m^{7}G$_{46}$ was based on previously described methods (Wintermeyer & Zachau, 1970; Simsek et al., 1973). A 1-mg sample of tRNA^{Phe} was dissolved in 1 mL of H_2O and dialyzed extensively against a solution of 1 M NaCl and 5 mM EDTA, followed by dialysis against deionized water to remove residual metal ions. A 1-mL aliquot of 0.1 N NaOH was added to the tRNA solution, and the resultant mixture was incubated for 15 min at room temperature. The pH was then adjusted to 4.5 by addition of 1/200 (v/v) glacial acetic acid. The tRNA^{Phe}–m^{7}G was precipitated with EtOH, and chain scission was carried out with aniline as described above. Resulting fragments 1–45 and 47–76 were purified by denaturing (6 M urea) 20% polyacrylamide gel electrophoresis. The fragments were located by UV shadowing over Merck Kieselgel 60F_{254} plates, excised, and extracted with 0.25 M NaOAc (pH 5.5).

Oligodeoxynucleotides. DNA probes were synthesized by the DNA Chemistry Laboratory (Cancer Core Facility, Beckman Research Institute of the City of Hope) and were purified by FPLC using a Pharmacia Mono Q HR 5/5 column as described (Cubellis et al., 1985). The concentrations of DNA and RNA polynucleotides were determined spectrophotometrically using the formula and data compiled by Borer (Borer, 1976). Extinction coefficients for DNA probes, ϵ_{260} (M^{-1} cm^{-1}; $\times 10^3$) were as follows: CGCTCTC, 54.7; GCTCTC, 48.2; GTCTGGC, 61.8; CCAGAT, 59.1; CTCCAGA, 67.0; CTCCC, 37.1; TCCAGA, 60.5.

5′ Labeling of RNA. All RNA fragments were 5′ end labeled with ^{32}P. A 20-pmol sample of RNA was dephosphorylated with 1 unit of calf intestine alkaline phosphatase in 10–20 μL of 1× CIP buffer. The reaction volume was brought to 50 μL and extracted 2× with TE-saturated phenol and 1× with Et_2O. After precipitation with EtOH and drying, the pellet was resuspended in 7 μL of H_2O, to which 1 μL of 10× T4 kinase buffer, 1 μL of [γ-^{32}P]ATP (specific activity 6000 Ci/mmol, ~20 mM), and 1 μL (10 units/μL) of T4 polynucleotide kinase were added. Following incubation for 30 min at 37 °C, another 10 units of kinase was added and the incubation was extended for 30 additional min. The reaction was then passed through a Sephadex G-25 column to remove unincorporated [γ-^{32}P]ATP and precipitated with EtOH. Labeled fragments were purified by polyacrylamide gel electrophoresis as described above.

Oligodeoxyribonucleotide-Directed RNAse H Cleavage of tRNA^{Phe} Half-Molecules. The RNAse H used in this work was either purchased from United States Biochemical or purified from an overproducing *E. coli* strain N4830 containing plasmid SK58 (a kind gift of Dr. R. J. Crouch) according to published procedures omitting a DNA–cellulose chromatography step (Arendes et al., 1982). Fractions were assayed for the production of acid-soluble material using poly(dT)·poly([^{32}P]rA) as substrate (Keller & Crouch, 1972). For the purposes of identifying the exact cleavage site and to determine optimal ratios of DNA to RNA for RNAse H digestion, analytical reactions were first conducted with 5′ end-labeled half-molecules. The reaction mixtures (5 μL) containing 40 mM Tris–HCl (pH 7.9), 4 mM $MgCl_2$, 6 pmol of RNA, and various amounts (6, 12, 30, or 60 pmol) of oligodeoxyribonucleotide were incubated for 3 min at 70 °C and allowed to cool to room temperature slowly. The volume was then brought to 10 μL by adding 4 μL of 50 mM Tris–HCl (pH 7.9), 5 mM $MgCl_2$, 2.5 mM DTT, and 450 ng of BSA. A 1-μL aliquot of diluted RNaseH fraction (~0.5–1.0 unit) was added, and the reaction mixtures were incubated for 1 h at 37 °C. Five microliters of 10 M urea containing 0.05% bromophenol blue and 0.05% xylene cyanol was added to the samples, and the mixtures were loaded onto a 20% polyacrylamide sequencing gel. It should be noted that the end products of the RNAse H reaction are 5′-phosphate and 3′-OH, while those for the RNAse T1 and Phy M reactions are 3′-phosphate and 5′-OH. Once the exact cleavage sites were identified, reactions were scaled up for preparative purposes. Total reaction volume was 1 mL. The RNA substrate (between 10 and 20 nmol) and the appropriate amount of oligodeoxyribonucleotides based on the analytical results were hybridized as described above. In general, a 1–2-fold excess of DNA probe was used for target sequences of single-strand RNA and a 5–10-fold excess for target sequences where a secondary structure likely exists. A total of 20–30 units of RNaseH were usually sufficient to

[1] Abbreviations: MPD, 2-methyl-2,4-pentanediol; EG, ethylene glycol; PEG, poly(ethylene glycol); EtOH, ethyl alcohol; MeOH, methanol; Et_2O, diethyl ether; TEAA, triethylammonium acetate, DTT, dithiothreitol; BSA, bovine serum albumin.

digest the substrates completely within 1–2 h. Reaction products were eluted on 20% polyacrylamide gels and visualized by UV shadowing as described above.

Calculated Extinction Coefficients of RNA Fragments. The extinction coefficients for RNA fragments were calculated according to the rules cited above (Borer, 1976). The values of ϵ_{260} (M^{-1} cm^{-1}; $\times 10^3$) are as follows: 1–36 (5′ half-molecule), 362.9; 1–24, 228.0; 1–30, 280.8; 1–45, 436.6; 38–76 (3′ half molecule), 382.7; 46–76, 299.1; 47–76, 287.8.

Pb^{2+} Cleavage Reactions. The standard reaction mixture for the lead-induced cleavage contains 10 μM Tris–HCl (pH 7.6), 10 mM $MgCl_2$, 0.2 mM spermine, and 50 μM $Pb(OAc)_2$. After the addition of substrate and catalytic RNAs, the reaction mixtures (5 μL) minus $Pb(OAc)_2$ were heated to 70 °C in a heat block and allowed to cool to room temperature. A 1-μL aliquot of 300 μM $Pb(OAc)_2$ solution was added, and the mixtures were incubated at the appropriate temperature. Reactions were quenched by the addition of 4 μL of a solution containing 10 M urea, 20 mM EDTA, 0.05% bromophenol blue, and 0.05% xylene cyanol. Reactions were analyzed on a 20% polyacrylamide sequencing gel (6 M urea). Quantitation of individual bands on the gel was performed using an Ambis Radioanalytic Image System (San Diego, CA), with corrections made for background (secondary cleavage).

Kinetic Determinations of Fragment Combinations. For measurements of k_{cat} and K_m, 0.3 μM of T-loop-containing ribozyme fragments was incubated with eight or nine different concentrations of 5′ ^{32}P-labeled substrate fragments, in excess from 0.6 to 9.0 μM. The cleavage rate for all fragment combinations except for those involving 1–24 as substrate was proportional to the concentration of T-loop-containing fragment during the first 5 min; hence the average velocity obtained during this time for these combinations was taken as the initial velocity. For reactions involving 1–24, linear concentration dependence occurred over the first 10 min. (Data not shown.) Each velocity determination was plotted as a line for a fixed value of s to yield direct linear plots, as described by Eisenthal and Cornish-Bowden (1974). The coordinates of the intersection of lines in the first quadrant yield direct estimates of K_m and V_{max}, with the median values corresponding to best estimates.

RESULTS AND DISCUSSION

Half-Molecule Reaction. The site-specific cleavage reaction is observed up to a temperature of ~70 °C. Above this temperature, almost all the 5′ half-molecule remains unreacted even after 4 h. Prolonged incubation (>12 h) at this temperature results in a random cleavage ladder. It is likely that the intermolecular contacts required for specific cleavage cannot form. This is supported by variable-temperature circular dichroism (CD) studies of a 1:1 mixture of half-molecules, which show a large structural transition at 70 °C consistent with melting. Since the substrate molecule was stable over time in the presence of Pb^{2+} at 50 °C, this temperature was chosen to study the reaction in detail.

Figure 1 shows the time course of reaction for the 5′ and 3′ halves in the presence of lead ions at 50 °C. It can be seen that at a ratio of 10:1 5′ half (1–36) to 3′ half (38–76) about seven turnovers have occurred after 4 h. The increase in cleavage fragment 1–17 is concomitant with the disappearance of starting material. About 60% conversion is observed. A minor cleavage at G_{15} is barely discernible after 2–4 h (lanes 8 and 9). This minor site, along with an additional cleavage at D_{16}, has been observed in the reaction of the intact molecule (Brown et al., 1985; Krzyzosiak et al., 1988) and occasionally

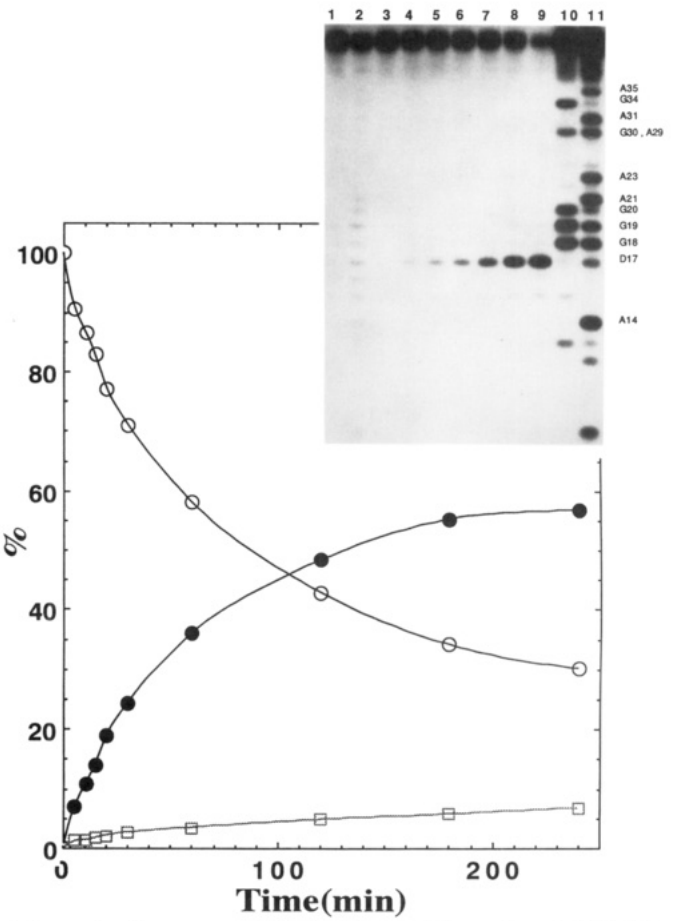

FIGURE 1: Time course of the lead-promoted reaction of $tRNA^{Phe}$ half-molecules 1–36 and 38–76. A 30-pmol sample of 5′ end-labeled 1–36 was incubated with 3 pmol of 38–76 in the presence of 50 μM $Pb(OAc)_2$: (●) the percentage of 1–17 primary cleavage product; (○) percentage of the 5′ half-molecule. The formation of secondary cleavage product 1–15 (□) is also shown. Inset: Lanes 1–3 are control reactions incubated for 4 h at 50 °C. Lane 1, 1–36 in the absence of lead ions and 38–76; lane 2, 1–36 plus $Pb(OAc)_2$; lane 3, 1–36 + 38–76 in the absence of $Pb(OAc)_2$; lanes 4–9, reactions incubated for 5, 15, 30, 60, 120, and 240 min, respectively; lanes 10 and 11, RNAse T1 (G) and Phy M (U+A) sequencing lanes.

appears in some of the fragment pairs that we studied, especially when T-loop-containing fragments are used in excess (see below). These sites were shown to be of secondary origin, and it is likely that this is also the case for the fragment recombination reactions.

Kinetics of the Half-Molecule Reaction. The observation of catalysis by the 3′ half-molecule and the demonstration of saturation with increasing substrate concentration (data not shown) prompted us to fit the rate data to the Michaelis–Menten approximation. Estimates of V_{max} and K_m were obtained from direct linear plots of the velocity data (Eisenthal & Cornish-Bowden, 1974). K_m was determined to be 5.1 μM, while the k_{cat} was found to be 0.58 min^{-1}. This value of k_{cat} is similar to that reported for a small hammerhead catalytic RNA system, yet the K_m is ~7.5-fold greater for the half-molecule reaction (Uhlenbeck, 1987). The dependence of the reaction velocity on temperature is presented in the form of an Arrhenius plot (Figure 2). The plot is biphasic over the temperature range of 16–55 °C, displaying an overall concave upward shape. The observation of a discontinuity in the Arrhenius plot implies two different reaction pathways characterized by two different energies of activation. Upward curvature reminiscent of that seen here has been documented for fumarase under alkaline (pH > 7.6) conditions (Massey, 1952). Although an exact physical interpretation of these

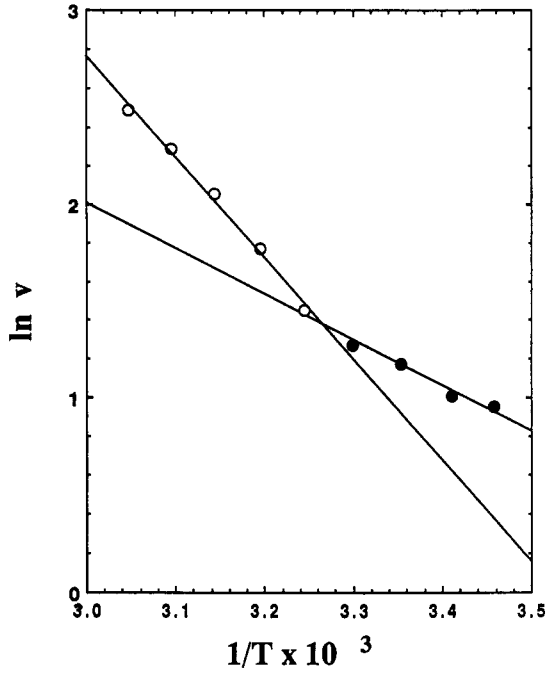

FIGURE 2: Arrhenius plot of the half-molecule reaction. Thirty picomoles of 1–36 and 15 pmol of 38–76 were incubated for 5 min in the standard reaction mixture at the indicated temperatures. The data yielded a biphasic plot, best fitted by two lines with correlation coefficients 0.983 (●) and 0.994 (○). The two values of E_a obtained are 10.39 kcal mol^{-1} between 33 and 55 °C (○) and 4.67 kcal mol^{-1} from 16 to 33 °C (●).

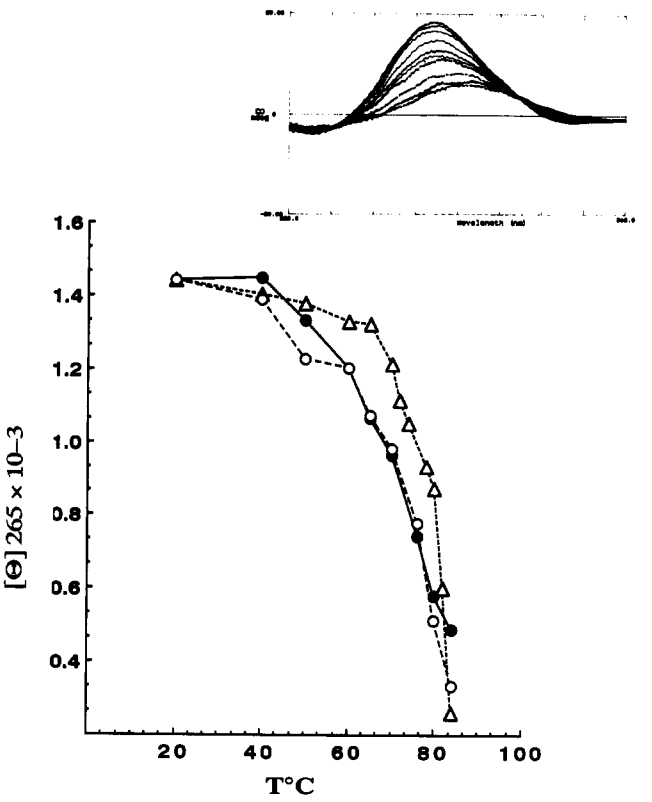

FIGURE 3: CD melting curves at 260 nm for tRNA^{Phe}, tRNA^{Phe}–Y, and 1–36 + 38–76. Solutions (12 μM) of the intact tRNA^{Phe} (△), tRNA^{Phe-Y} (○), and a 1:1 mixture of half-molecules (●) were scanned from 210 to 310 nm at various temperatures on a Jasco J-600 spectropolarimeter. The molar ellipticity at 265 nm was then plotted as a function of temperature. CD spectra from 210 to 310 nm for the intact tRNA^{Phe} as a function of temperature are shown in the inset.

data is difficult, a number of explanations seem plausible. One is that there are two unique activated ES complexes which can result in cleavage at D_{17} and that these critical complexes possess different energies of activation. These might be two complexes which differ in ligand geometry about the lead ion, for example. This situation would give rise to an activation energy increase with increasing temperature, as shown in Figure 2 (Dixon & Webb, 1979; Kistiakowsky & Lumry, 1949).

CD Studies on the Recombined Fragments 38–76 and 1–36. The question arises as to whether the half-molecule reaction occurs via an intermediate resembling the native molecule. Monitoring the circular dichroism absorbance at 265 nm as a function of temperature provides a sensitive probe of RNA structure (Prinz et al., 1974). A plot of the molar ellipticities at 265 nm for a 1:1 mixture of half-molecule fragments, tRNA^{Phe}–Y and the native molecule as a function of temperature is shown in Figure 3. Ionic conditions were exactly as described in Materials and Methods for the fragment reactions, with the omission of Pb^{2+}. It can be seen that the intact tRNA^{Phe} molecule undergoes a large structural transition at ~70 °C; further temperature increases produce a curve characteristic of an unstacked random coil conformation. Comparison of this curve with that of a 1:1 mixture of half-fragments shows the latter to possess a somewhat broader melting profile, with a lower transition temperature. It is also seen that the CD melting curve of the recombined half-molecules is virtually superimposable upon the tRNA^{Phe}–Y profile. We thus conclude that the reconstituted half-fragments of tRNA^{Phe} adopt a structure that is probably the same as that of the tRNA^{Phe}–Y molecule and that the stacked Y base contributes significantly to the stability and thus the observed melting transitions of the native tRNA^{Phe} molecule.

The effect of Y-base removal on the stability of tRNA^{Phe} has been examined by NMR. Specific lowering of temperature-induced transitions was found for residues T_{54}, $^2_2mG_{26}$, and D_{16} (Davanloo et al., 1979) when the Y base was removed. These positions are quite distal to the Y base and flank the cleavage site. Long-range conformational effects had been previously demonstrated by complementary oligonucleotide binding to tRNA^{Phe}, which showed that Y-base removal could effect the binding of tetranucleotides to the D-loop (Cameron & Uhlenbeck, 1973). Most significantly, the tRNA^{Phe}–Y molecule has been found to undergo lead-catalyzed self-cleavage at a faster rate than the native molecule (Krzyzosiak et al., 1988), perhaps reflecting a geometry about D_{17} more susceptible to cleavage, a situation likely reflected in the half-molecule reaction.

Dissection of tRNA Half-Molecules by RNaseH. RNA cleavage using RNAse H requires the formation of an RNA:DNA heteroduplex, most conveniently generated for these purposes using small DNA oligonucleotides (Donis-Keller, 1979). One problem encountered in using RNAse H and deoxyoligonucleotides in the dissection of RNA substrates is the uncertainty in predicting the exact location of RNA cleavage within the heteroduplex, although cleavage invariably occurs toward the 3′ side of the RNA. In our experience we have rarely encountered more than three cleavage sites within a heteroduplex, and this seems to be in accord with a survey of literature examples of *E. coli* RNAse H activity (Donis-Keller, 1979; Stepanova et al., 1979; Inoue et al., 1987; Lorenz et al., 1987). One site sometimes predominates (see below), but it is usually a relatively simple matter to obtain preparative amounts of the desired RNA in acceptable yields. We have used the *E. coli* enzyme exclusively in this work. The structure of this enzyme has recently been elucidated by X-ray diffraction (Yang et al., 1991; Katayanagi, et al., 1990).

Using DNA probes of five to seven bases, both T- and D-loop-containing halves were further dissected into smaller

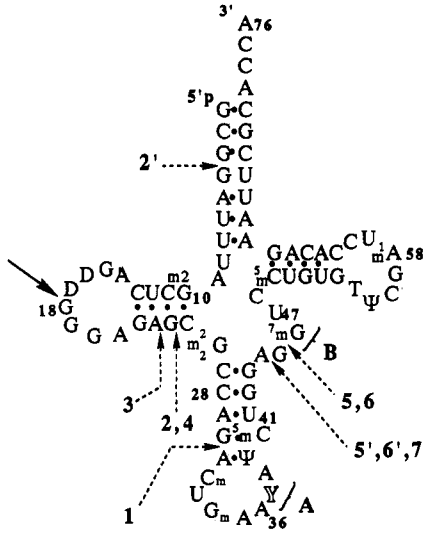

Parent Molecule	Cleavage Site	Fragment Isolated	DNA Probe
1-76	A	1-36, 38-76	-
"	B	1-45, 47-76	-
1-36	1	1-30	GTCTGGC
"	2,2'	1-24,4-24	CGCTCTC
"	3	1-23	CTCCC
"	4	1-24	GCTCTC
38-76	5,5'	46-76, 45-76	CTCCAGA
"	6,6'	" , "	TCCAGA
"	7	45-76	CCAGAT

FIGURE 4: Map of yeast $tRNA^{Phe}$ indicating points of cleavage by chemical and enzymatic methods. Numbers refer to RNAse H cleavage sites and the DNA probes used to create them. Primes denote secondary cleavage sites (>5%; see text). A and B (bracketed sites) denote bases removed by chemical excision to create the indicated fragments. A solid arrow denotes the Pb^{2+} cleavage site, while dotted arrows designate RNAse H cleavages. Tertiary base pairs found in the native structure: m^1A_{58}–T_{54}, C_{56}–G_{19}, Y_{55}–G_{18}, U_8–A_{14}, A_9–A_{23}, C_{48}–G_{15}, m^7G_{46}–G_{22}, G_{45}–m_2G_{10}, A_{44} – $m_2^2G_{26}$. Some or all of these interactions may exist in the recombined fragments.

pieces by RNAse H. A map of the fragments used in this study and the DNA probes used to obtain them are shown in Figure 4. Reactions were run on an analytical scale using a 5′ ^{32}P-labeled fragment in order to ascertain the extent and location of the cleavage and to permit sequencing of the isolated fragments. Reactions were then carried out on a preparative scale, and fragments were isolated as described in Materials and Methods. The 1–30 fragment was obtained relatively cleanly, with the predominant cleavage site located two bases toward the interior of the heteroduplex from the 3′ side of the RNA. Minor cleavages (<5%) were found to occur ±1 base from the major cleavage site. Substrate fragment 1–24 could be isolated cleanly using hexamer GCTCTC (**4**).

The heptamer probe CGCTCTC (**2**) similarly directed cleavage at G_{24}, but an additional fast-running end-labeled fragment appeared near the gel front. UV shadowing of the preparative reactions showed two closely running bands. The faster migrating band was isolated, 5′ end-labeled, and sequenced. This fragment, comprising ~40% of cleaved products, contained nucleotides 4–24. It is probable that the CGC end of the heptamer probe hybridized to the 5′-GCG of the 5′ half-molecule, producing a heteroduplex of three nucleotides sufficient to signal recognition and cleavage by RNAse H. No 4–36 fragment is produced, and it is likely that secondary cleavages are observed because an excess of probe is used in these reactions. Removing the 5′ C from the heptamer, which would shorten the postulated secondary heteroduplex to only two nucleotides, results only in cleavage at the desired G_{24}. Hexamer probe **4** readily disrupted the D-stem and enabled RNase H cleavage to occur precisely after G_{24}, with no additional cleavage sites detected by autoradiography of the 5′ end-labeled 5′ half-molecule or by UV shadowing of the preparative reaction products. Fragment 1–23 was generated using probe **3**. We were unable to obtain cleavage at C_{25}. This failure may be due to the presence of a non-Watson–Crick base pair between $^2_2mG_{26}$ of $tRNA^{Phe}$ and the 5′ terminal C of oligonucleotide **2**. RNAse H may not be able to recognize and/or cleave at this base pair. Not all modified bases were resistant to RNAse H cleavage. Reaction at m^7G_{46} to produce fragment 46–76 proceeded in good yield. The fact that cleavage can occur at m^7G_{46} in 38–76 but not at $^2_2mG_{26}$ in 1–36 raises the possibility that methylation at N2 interferes with the activity of RNAse H.

Cleavages of the variable loop region via heteroduplexes formed from the isolated 3′ half-molecule show similar effects. Cleavage by RNAse H solely after G_{45} was found to occur when the heteroduplex formed from hexamer **7** was preequilibrated with the 3′ half. A related hexamer, TCCAGA (**6**), which extends the heteroduplex one base in the 3′ direction of the RNA target, shifts the major RNAse H cleavage site from G_{45} to m^7G_{46}, producing 46–76 and 45–76 in a 60:40 ratio. Exactly the same cleavage pattern is obtained with CTCCAGA (**5**), producing cleavages both interior and adjacent to the heteroduplex.

The cleavage efficiency of RNAse H was found to be dependent on the stoichiometric ratio of DNA probe:RNA substrate. Cleavage efficiency generally increased with increasing amount of DNA probe. Hybridization of **4** to the 5′ half-molecule requires disruption of the D-stem and can be made thermodynamically more favorable by the addition of excess, resulting in a larger heteroduplex substrate population. A similar effect is seen upon increasing up to 10-fold the amount of probe **1** over 5′ half-molecule to produce 1–30, except that in this instance the target RNA is a single-stranded rather than a stem–loop structure. Minor cleavage sites at A_{29} and A_{31} appear when probe **1** is used, although with increasing amounts of DNA the A_{29} site becomes the predominant minor site, whereas with lower amounts of probe A_{31} is the favored minor site.

Attempts to dissect the intact molecule in this way were not very successful, perhaps due to the barriers to hybridization provided by tertiary folding. Hybridization of an oligonucleotide complementary to bases 30–36 in the intact $tRNA^{Phe}$ and treatment with RNAse H produced a weak cleavage at A_{36} (<10%). It is not clear in this case whether the adjacent Y base affects the RNAse H recognition and/or cleavage event or whether this hypermodified purine base interferes with the DNA hybridization step. In this regard, the effects of modified bases, non-Watson–Crick base pairings, and local RNA structure on heteroduplex formation and subsequent RNAse H cleavage require further study.

Single-Turnover Reactions of Fragment Combinations. The goal of the next set of experiments was to determine the minimum structural requirements for the intermolecular lead cleavage reaction. Substrate fragments 1–36, 1–30, 1–24, and 1–45 were combined with catalytic RNA fragments 38–76, 46–76, and 47–76 in all possible combinations, yielding 12 reactions (Figure 5). Since turnover is not possible in these experiments, what we observe only reflects the relative

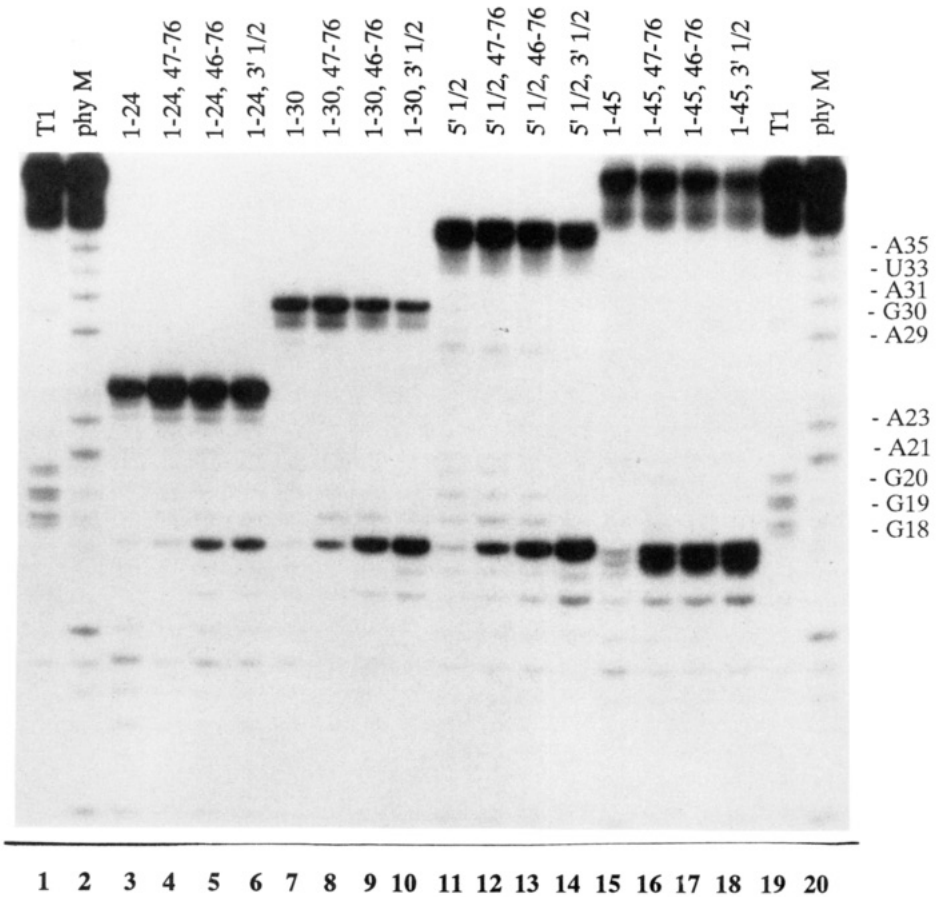

FIGURE 5: Pb^{2+}-promoted cleavage reactions of recombined tRNA^{Phe} fragments. Three picomoles of 5′ ^{32}P-labeled D-loop-containing substrate fragments 1–24, 1–30, 1–36, and 1–45 were incubated with and without 6 pmol of T-loop-containing ribozyme fragments 38–76, 46–76, and 47–76 as indicated. Reactions contained 50 μM $Pb(OAc)_2$ and were allowed to react for 1 h at 37 °C.

ability of a particular combination to acquire a cleaving conformation in the presence of lead. Although in some lanes background cleavage is observed, a new major cleavage site is never created with any fragment combination. Lanes, 3, 7, 11, and 15 consist of the various substrate fragments incubated with 50 μM Pb^{2+} in the absence of any T-loop-containing fragment. It can be seen that some nonspecific cleavage occurs. Prolonged reaction of the substrate with [Pb^{2+}] (> 50 μM) results in the generation of a cleavage ladder. The background cleavage using the conditions described in Figure 5 does not increase appreciably even after 16 h of incubation. Lanes 4–6 show the reactions of the 1–24 substrate fragment with three T-loop-containing fragments. Fragment 1–24 is cleaved only slightly by 47–76, with cleavage at D_{17} marginally above background. Using a fragment that is longer by only a single residue, m^7G_{46}, results in a marked improvement in cleavage (lane 5). Longer T-loop fragments, such as 38–76 do not appreciably enhance the cleavage of 1–24 (lane 6), indicating that when 1–24 is the substrate fragment, the presence of nonbonding residues beyond m^7G_{46} does not affect the cleavage efficiency under single-turnover conditions. This identifies a potential minimum cleavage complex consisting of 1–24 and 46–76.

Lanes 7–10 show the results of experiments using 1–30 as substrate. In contrast to the situation observed with 1–24, 47–76 RNA competently cleaves this substrate (lanes 4 vs 8). Fragment 1–30, unlike 1–24, contains a complete D-stem. This suggests that substrates containing a stable D-stem are cleaved more efficiently and that any interactions which can stabilize this helix might be expected to result in enhanced cleavage. Perhaps a closed D-stem facilitates the interactions between T- and D-loops required for cleavage. The 46–76 fragment cleaves 1–30 at least ~3-fold and more effectively, a trend also seen with the 1–24 fragment as substrate (compare lanes 8 and 9). The combination of fragments 1–30 and 38–76 has the potential to yield a structure possessing an anticodon stem upon annealing. It is not surprising that this combination yields a cleavage reaction which is similar to the half-molecule reaction in relative cleavage efficiency. The reactions of the 5′ substrate half-molecule are depicted in lanes 11–14. The 47–76 fragment cleaves the 5′ half-molecule (lane 12), although again not as effectively as 46–76 (lane 13). Lane 14 is the reaction of 5′ and 3′ half-molecules at 37 °C. The minor cleavage sites at D_{16} and G_{15} also observed in the autocleavage of the intact molecule are apparent. Excess of ribozyme is probably a factor in the generation of secondary cleavages in these experiments.

Lanes 15–18 present results obtained with 5′ substrate fragment 1–45, produced by chemical excision of m^7G_{46}. This was the only substrate examined that contained both the D- and anticodon stem–loops. The addition of the anticodon stem and loop to the substrate seems to dramatically affect the D-loop cleavage. As shown in lane 16, cleavage of 1–45 by 47–76 is quite strong, suggesting that the anticodon influences the geometry about the cleavage site. This substrate fragment appears to be cleaved to the greatest extent under single-turnover conditions by the three catalytic RNA fragments. Of particular interest is the reaction of the 3′ half-molecule 38–76 with the 1–45 substrate (lane 18). A complex formed from these two fragments would have a redundancy of bases 38–45, allowing for several possible base-pairing arrangements about the anticodon stem.

A number of fragment combinations not shown in Figure 5 failed to yield site-specific cleavages when combined with Pb^{2+} under our standard reaction conditions. A fragment containing residues 1–23 was degraded nonspecifically by a

2-fold excess of either the 5′ half-molecule or the 46–76 ribozyme fragment in the presence of 50 μM Pb^{2+} at 37 °C. If a stable D-stem is a prerequisite for specific cleavage at p18, as discussed above, perhaps a minimum of three base pairs (possible for 1–24 but not 1–23) is needed to maintain the correct loop conformation for cleavage at 37 °C. A substrate fragment 4–24 proved highly resistant to hydrolysis by the 46–76 fragment in the presence of 50 μM Pb^{2+} at 37 °C and was recovered uncleaved after several hours of incubation. This seemed to imply that association between the two fragments was not occurring and also that there were no Pb^{2+} binding sites on the fragment 4–24 which could lead to autohydrolysis.

The loss of the terminal 5′-GCG residues from 1–24 to create the 4–24 fragment would leave four bases available for pairing with the 3′ half derived fragment to form a truncated acceptor stem upon association. The first base pair in this hypothetical intermediate would consist of the G:U wobble pair. If a successful cleavage reaction requires as a first step association of the two single strands comprising the acceptor stem as a nucleation event for the formation of the required tertiary bonds, then failure to achieve a stable stem at this temperature (37 °C) would prevent cleavage. Time-resolved melting studies indicate that the acceptor stem is the first secondary structural feature to melt, while the T- and D-stems are the most stable (Riesner et al., 1973; Boyle et al., 1983). Hence it is plausible that a truncated acceptor stem would not form at the reaction temperature. Lower temperatures were not investigated for this combination, although it might be of interest to see whether a cleavable complex can be formed under certain conditions. Ribozyme fragments missing the entire variable loop, such as 49–76 or 48–76, were not examined. Since 47–76 cleaved 1–24 rather poorly, these shorter ribozyme fragments would not be expected to yield site-specific reactions with the minimum substrate. Although a 47–76 ribozyme competetently promoted the cleavage of substrates 1–30 and larger, the smallest *combination* that demonstrated efficient intermolecular cleavage was the 1–24 D-loop fragment and the 46–76 T-loop fragment. We will call this system the minimum complex, although 2–24 and 3–24 might be competently cleaved.

Kinetic Analysis of the Catalytic Cleavage Reactions of Fragment Combinations. Table I displays the values of k_{cat} and K_m obtained for all site-specifically cleaved fragment combinations under catalytic conditions. Measurements were also made of the initial rates in order to detect deviations from steady-state behavior. For purposes of comparison, the table is arranged in decreasing order of k_{cat}'s and initial rates. An examination of the rates in Table I reveals a 25-fold difference in measured k_{cat}'s, and an 18-fold variation in initial rates. K_m's vary by only 3-fold, and differences in catalytic efficiency are reflected for the most part by differences in k_{cat}. All the kinetic measurements were made at 37 °C, using identical reaction conditions. This temperature was chosen as a standard reaction condition because some of the combinations of smaller fragments yielded less specific reactions at temperatures of >40 °C in the presence of lead ions (see Figure 6). The fastest turnover number measured at 37 °C was 0.1 min^{-1}. This can be compared with a value of 0.5 min^{-1} obtained with the half-molecule combination at 50 °C. The fastest turnovers were measured for reactions of catalytic RNA fragments cleaving the 1–45 substrate. The slowest reactions observed were those that involved the combination of the smallest fragments. Several effects can be deduced from a study of the rate data which point to the influence of tertiary base pairs, substrate stem–loop stability, single-stranded flanking sequences, and secondary structural features remote from the reaction center on the cleavage rate.

Table I: Kinetic Parameters for the Catalytic Reactions of the $tRNA^{Phe}$ Fragment Combinations[a]

E	S	K_m (μM)	k_{cat} (min^{-1})	k_{cat}/K_m ($\times 10^4$)
47–76	1–45	1.7	0.117	6.86
46–76	1–45	1.2	0.089	7.18
38–76	1–30	2.3	0.085	3.69
38–76	1–45	1.8	0.078	4.35
38–76	1–36	1.2	0.053	4.41
46–76	1–36	1.4	0.042	3.11
47–76	1–36	3.1	0.040	1.29
38–76	1–24	1.1	0.036	3.61
46–76	1–30	1.1	0.019	1.37
46–76	1–24	1.0	0.017	1.68
47–76	1–30	0.9	0.014	1.55
47–76	1–24	0.8	0.005	0.58

	Initial Rates[b]	
E	S	rate
46–76	1–45	21.8
47–76	1–45	21.2
38–76	1–36	20.4
38–76	1–45	19.9
46–76	1–36	12.4
38–76	1–30	10.5
46–76	1–30	9.22
47–76	1–30	4.66
47–76	1–36	4.28
38–76	1–24	2.75
46–76	1–24	2.19
47–76	1–24	1.24

[a] Best estimates of K_m and V_{max} were obtained by direct linear plots of the data as described in Materials and Methods. Each value in the table represents the best estimate from two determinations. All reactions except for those invoiving 1–24 as substrate were allowed to proceed for 5 min at 37 °C. Reactions of 1–24 were stopped after 10 min. [b] Initial rate given as nanomoles of substrate (S) cleaved per minute for 3 pmol of enzyme at 37 °C. Initial rate determinations were made with a 2-fold excess of substrate fragments; measurements were taken at 5 and 10 min, and values are the average of three determinations.

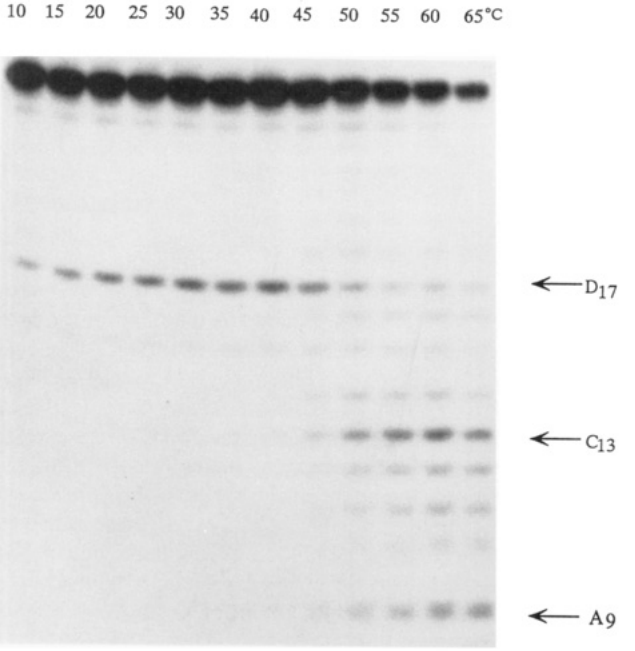

FIGURE 6: Effect of temperature on the minimum reaction. Three picomoles of 46–76 and 6 pmol of 5′ ^{32}P-labeled 1–24 were incubated at the indicated temperatures for 10 min. Sites of major cleavage are indicated by arrows.

Tertiary interactions involving the variable loop and D-stem can influence the kinetics of cleavage for some combinations. In particular, it can be seen how the tertiary base pairs m^7G_{46}–

G_{22} and G_{45}–m^2G_{10} influence the cleavage in the absence of the anticodon stem. Comparisons of k_{cat}'s, initial rates, and efficiencies for the cleavage of 1–24 by 47–76, 46–76, and 38–76 show a gradual enhancement as one increases the number of potential tertiary interactions involving the variable loop from one to three. For example, the steady-state turnover rates are found to be 0.005, 0.017, and 0.036 min^{-1}, respectively. Fragment 47–76 cleaves the least effectively. This combination is characterized by the slowest rates we have measured for the reactions of tRNA^{Phe} fragments. Only one tertiary interaction involving the variable loop, C_{48}–G_{15}, is possible in this fragment combination. The extremely poor turnover for this reaction may indicate that the complex between fragments forms only weakly ($K_d \gg K_a$) or that the tertiary interactions between fragments are not sufficient to allow cleavage by lead. The former possibility can be disregraded by noting that the Michaelis constants for cleavage of 1–24 by 47–76 and 46–76 are nearly the same; yet the reaction with 46–76 possesses a 3-fold higher k_{cat}. Unusually slow product dissociation is probably also not a factor in the poor turnover rates observed. That the proper transition-state geometry cannot be achieved is consistent with the results shown in Figure 5, where even a 2-fold excess of 47–76 results only in a barely discernible cleavage of 1–24. The additional interaction provided by m^7G_{46} is apparently enough to enable adequate rates of turnover. The rate differences observed argue that tertiary interactions found in the intact molecule may be reconstituted in fragment combinations.

Variable loop nucleotides which can form base triplets with the D-stem of the 1–24 fragment may affect the cleavage efficiency by allowing more precise alignment of D- and T-loops in the transition state. The 38–76 fragment is capable of maintaining all the variable loop interactions with the D-stem–loop that are found in the native molecule. An additional tertiary interaction, m^2G_{10}–G_{45}, not possible for the 46–76 catalyst fragment combinations, can potentially affect the rate in this case. Although it is not clear whether this bonding arrangement can form in the absence of the C_{25}–m^2G_{10} base pair, the increase in rate may reflect the presence of this interaction for the catalytic cleavage of 1–24 by 38–76. The origins of rate differences between combinations which possess single-stranded regions (e.g., 46–76 with 1–30 and 1–36) are unclear at this point and must await further experimentation. In addition to the possibility of long-range conformational effects, the influence of electrostatic repulsion on the observed turnover rates should be considered.

The fastest and most efficient reactions at p18 involved substrate fragments which also contained an intact anticodon stem–loop. As we have demonstrated above, no elements of the anticodon are required for cleavage, yet the presence of even some of these elements enhances the observed rate. The 1–45 substrate fragment is cleaved the fastest, as shown by initial and steady-state rate determinations and catalytic efficiencies. Easily generated by base-catalyzed excision of m^7G_{46}, 1–45 has been studied by NMR and temperature-jump experiments and shown to be highly ordered, retaining the helical arrangement of D- and T-stems found in the intact molecule (Boyle et al., 1980, 1983). Interestingly, the $^2mG_{26}$ – A_{44} tertiary interaction can be identified in the NMR, whereas other possible tertiary arrangements for 1–45 that occur in the intact molecule such as U_8–A_{14} and the U_9–A_{23}–U_{12} base triple are not found. When the 46–76 and 47–76 catalytic RNA fragments are paired with this substrate, the best kinetic rates are observed, and thus these fragments can catalyze both the fastest and slowest reactions we were able to measure at 37 °C.

It is probably true to some extent that since only a few hydrogen bonds need to be broken and formed during each catalytic cycle, turnover is relatively efficient. But the numbers of bonds which need to be broken in order to effect catalyst release are the same as those required for the reaction of 46–76 and 47–76 with 1–24 or 1–30, reactions which possess substantially lower k_{cat}'s and initial rates. Substrate conformation may be the dominant effect in the reactions of 1–45 with 46–76 and 47–76. A favorable transition-state geometry for these fragment combinations could have been predicted from the results in Figure 5, lanes 17 and 18, where extensive cleavage is found to occur under single-turnover conditions, although the catalytic efficiency of these combinations could not have been predicted from those results alone. The differences seen between the reaction rates of 1–45 with 47–76 and 46–76 are negligible. This is in striking contrast to the kinetic results obtained with the shorter substrates, such as 1–24. Thus, while the formation of the base triple involving m^7G_{46} can enhance the cleavage of small substrates, this interaction can become unimportant if the substrate can be preorganized for efficient cleavage by folding.

We found the cleavage of 1–45 by the 3′ half-molecule to be of interest in view of the structural redundancy about the anticodon stem–loop and part of the variable loop. This reaction appears kinetically similar to the reactions of 47–76 and 46–76 with 1–45. This seems reasonable since it is unlikely that residues 45–38 of the 3′ half-molecule are not required for the reconstitution of a "nativelike" structure in trans. The k_{cat} which characterizes the cleavage of 1–45 by 47–76 is more than 2-fold greater than the value which characterizes the half-molecule reaction at 37 °C. The initial rates for these reactions are nearly the same. The half-molecule reaction appears to slow somewhat as the 3′ catalytic half-molecule becomes saturated with substrate, its k_{cat} falling to approximately the mean value of those reported in Table I (0.049 min^{-1}). Product dissociation may be rate limiting at 37 °C in this case. A greater degree of hydrogen bond and base-stacking reorganization is required for turnover in the half-molecule reaction as compared with the cleavage of 1–45 by 47–76. Alternatively, product inhibition or a fall in substrate concentration as the reaction proceeds toward saturation may also account for this effect in the half-molecule reaction.

It is also of interest to compare the rates of the half-molecule reaction at 37 °C with those described previously at 50 °C. Although initial rates were not determined at 50 °C, the k_{cat} for the reaction at this temperature is nearly 1 order of magnitude greater. Yet K_m is found to increase to the extent that the overall efficiency of the reaction at the higher temperature is only 2.5-fold enhanced. The reaction at higher temperature should possess an elevated rate of helix exchange relative to the reaction at 37 °C; hence an increase in the steady-state rate might be expected. The increase in K_m might be the result of fewer productive (i.e., resulting in cleavage) collisions between substrate and ribozyme at the elevated temperature.

The poor catalytic efficiency of most of the reactions led us to wonder whether conditions could be found that would substantially improve the rates of selected reactions. This would enable us to explore the catalytic potential of at least some of these tRNA^{Phe} fragments. We chose to focus on the "minimum" complex, 46–76/1–24. This combination is of particular interest since a three-helical arrangement reminiscent of that found in the hammerhead cleavage reaction is possible. The effects of temperature, added alcohols, and organic amines on the reaction rate were examined in detail.

Temperature Dependence of the Minimum Catalytic Cleavage Complex. The components of the minimum reaction were allowed to react for 10 min with 50 μM Pb^{2+} at various temperatures, the results of which are displayed in the autoradiograph of Figure 6. It can be seen that some cleavage is apparent even at 10 °C. The amount of cleavage product 1–17 increases slowly until temperatures of ~40 °C are reached, at which point the cleavage reaction becomes less specific. These cleavages are not entirely random, since sites at C_{13} and A_9 appear to predominate at temperatures of >45 °C. It cannot be determined from the use of 5′ end-labeled 1–24 alone whether these are secondary or primary cleavages of the substrate fragment. If however cleavage at C_{13} and A_9 were the result of secondary reactions, one would expect to see some cleavage at D_{17} by analogy with what is observed for the native $tRNA^{Phe}$. Similar behavior is also found for intermolecular reactions when T-loop-containing fragments are used in excess (D_{16} and G_{15} always appear as minor bands flanking the primary site; see Figure 5). The cleavage at C_{13} and A_9 and, to a lesser extent, C_{11} and U_{12} is particularly apparent at 65 °C. The result at this temperature is curious since normal cleavage at D_{17} is almost entirely absent. Nucleotides 9–13 comprise the upper half of the D-stem, while positions corresponding to the lower half 18–23 seem not to be hydrolyzed at all. The cleavage observed in this case does not resemble the high-temperature reaction of the 5′ half-molecule with Pb^{2+}, where a cleavage ladder is obtained. It is possible that an intermolecular cleavage reaction involving a open D-stem intermediate is occurring or that autohydrolysis of the 1–24 fragment is occurring from a nonrandom conformation. The reaction temperature optimum for cleavage at D_{17} of the 1–24/46–76 complex was taken as 37 °C.

Effects of Cosolvents and Polycations on the "Minimum Complex" Cleavage Rate. The many reports in the literature on the stimulatory effect of added cosolvents on the rates of enzymatic processes involving nucleic acids prompted us to examine this phenomenon for the lead cleavage reaction. Well-characterized examples of the so-called "excluded-volume effect" have been described for catalytic RNA reactions. For example, 15% PEG was reported to enhance the M1RNA cleavage of pre-$tRNA^{Tyr}$ by 5-fold, while a 2-fold enhancement was found upon the addition of 10% EtOH; 30% EtOH was found to inhibit the reaction (Guerrier-Takada et al., 1986). The effect of addition of volume-excluding solvents on the reaction of the minimum complex 1–24/46–76 was examined by titration. Approximately 4% cleavage is observed in the absence of alcohol when the reaction conditions are identical to those depicted in Figure 5. Modest amounts of most added alcohols have a stimulatory effect on the rate of cleavage at D_{17} over a fairly narrow range, resulting in a bell-shaped concentration vs percent cleavage profile. This cleavage enhancement in all cases was observed at alcohol concentrations well below the level at which precipitation of RNA is found to occur (<50% v/v) (Steely et al., 1986). When 5% MPD is added to the reaction, a nearly 9-fold improvement in cleavage efficiency is observed. Ethylene glycol is also stimulatory, although to a lesser extent. Ethanol and methanol are similar in their effects, although the former allows a 10-fold enhancement at a lower added concentration. PEG 6000 is completely inhibitory at all added concentrations and is capable of suppressing background cleavage even after extensive incubation with Pb^{2+} ions. The effect on enzymatic reactions by the addition of noninteracting solutes has been well documented [for reviews, see Minton (1981, 1983)]. The observed changes in rates can be the result of shifting of conformational equilibria between different forms of the enzyme, increases in the degree of association among reaction components, and equilibrium-independent enhancement of the specific activity of the enzyme. All of these can occur in the absence of direct interaction between added solute and the reaction components and depend only on the volume occupied by solute.

The effect of the polyamines spermine, spermidine, and putrescine in the presence of 15% EtOH on the cleavage efficiency was examined. Only for spermine is the effect stimulatory, maximal at 0.1 mM, yielding a 10% enhancement. The shorter polyamines spermidine and putrescine are inhibitory at all concentrations. In the absence of alcohol, the effect of added amines was small, with enhancements of only 1–3% observed for spermine at an optimal concentration of 0.5 mM. Concentrations greater than this impeded the cleavage reaction. This suggests possible cooperativity between spermine and ethanol in the enhancement of the cleavage reaction.

The binding of spermine to $tRNA^{Phe}$ has been analyzed in detail by X-ray crystallography (Quigley et al., 1978). It is possible in the present case that the interaction of 1–24 and 46–76 might be stabilized in a manner resembling the arrangement found in the intact molecule, with spermine bridging phosphates 9, 10, and 11 to 47, 46, and 45. Spermine is not required for the reaction, however, and the enhancement is only modest. An increase in cleavage efficiency upon the addition of spermine has been reported for a hammerhead catalytic RNA, where it was found that 0.5 mM spermine lowered the concentration of divalent cations required for efficient cleavage (Dahm & Uhlenbeck, 1991).

Kinetic Characterization Of the Minimum Complex. The catalytic properties of the minimum complex in the presence of 15% EtOH and 0.1 mM spermine at 37 °C were examined. A progress curve obtained for this reaction over a 4-h period is shown in Figure 7. The autoradiograph that represents these data is shown in the inset. At least seven turnovers are seen to occur, and 72% of the starting material is cleaved after 4 h. Direct linear plots of the reaction velocities yielded values of 2.6 μM and 0.21 min^{-1} for K_m and k_{cat}, respectively. An Arrhenius plot of the reaction is shown in Figure 8. Velocities were obtained over a range of 10–37 °C. At $T > 37$ °C, cleavage at D_{17} decreases (Figure 6); thus we were unable to measure velocities over the range of temperatures that was possible for the half-molecule reaction. An activation energy of 12 kcal mol^{-1} is reminiscent of that found for the half-molecule reaction in the upper range of temperatures. (33–55 °C)

These values can be compared to those in Table I for the minimum complex at 37 °C in the absence of alcohol. The reaction conditions were identical in every respect save for the addition of 15% EtOH and 100 μM spermine; thus, the kinetic differences reflect only the combined effect of these solutes. The overall efficiency of the reaction is increased by 3.4-fold, with an order of magnitude increase in k_{cat} offset somewhat by an increase in K_m from 0.7 to 2.6 μM. This situation is reminiscent of the enhancement in efficiency found for the half-molecule reaction when the temperature was increased from 37 to 50 °C, where an increase in k_{cat} was accompanied by a 4-fold increase in K_m. The increase in the observed K_m upon addition of alcohol may be related to the effect of increasing temperature in that a partial denaturation of the reaction complex may be occurring (Prinz et al., 1974).

CONCLUDING REMARKS

We have demonstrated the extent to which the Pb^{2+}-promoted self-cleavage reaction of the native $tRNA^{Phe}$ from

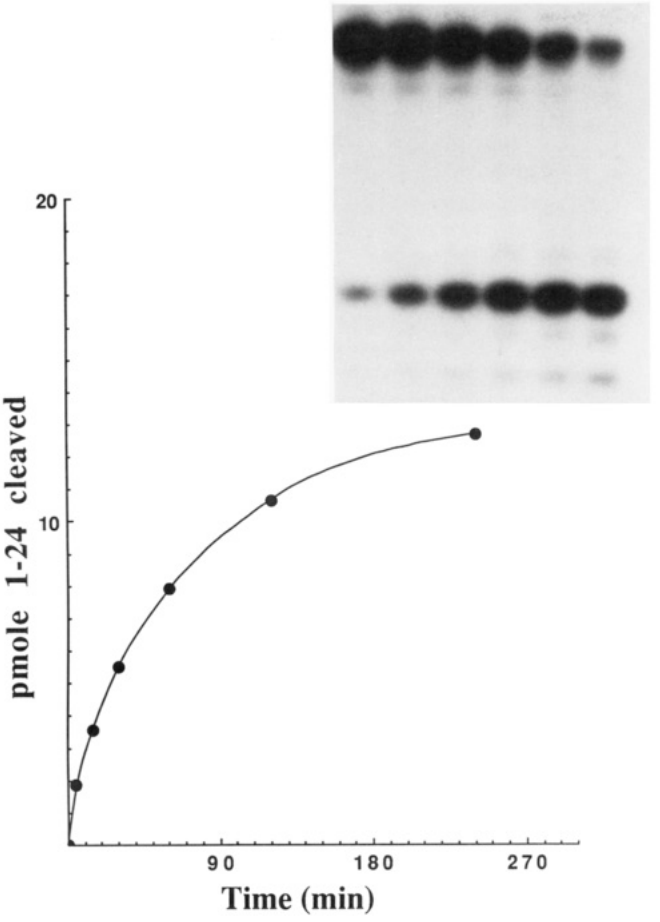

FIGURE 7: Time course of the reaction of 18 pmol of 1–24 substrate fragment with 1.8 pmol of 46–76. The amount of cleavage in the presence of 15% EtOH and 0.1 mM spermine was determined at 5, 15, 30, 60, 120, and 240 min, respectively.

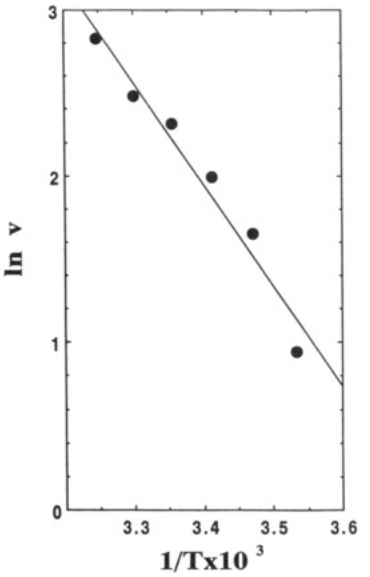

FIGURE 8: Arrhenius plot of the temperature dependence of the minimum complex in the presence of 15% EtOH and 0.1 mM spermine. E_a = 12 kcal mol^{-1}, R^2 = 0.96.

yeast can be made to occur in an intermolecular fashion, and that a rather small number of interactions between fragments are sufficient for site-specific cleavage. These results clearly indicate that the reaction is T-loop dependent, since cleavage was only observed in the presence of T-loop-containing fragments. Site-specific reactions invariably occurred at p18 when Pb^{2+} was used as the metal cofactor. Tertiary interactions involving the variable loop can have significant effects on the rate of reactions involving small substrates containing only a partial D-stem. These effects become unimportant for the 1–45 substrate, presumably because this fragment is preorganized for cleavage by folding. Catalytically nonessential flanking sequences can also modify the reaction rate.

Other tRNAs have been observed to undergo site-specific cleavage by lead ion. Interestingly, cleavage at p18 is also the major cleavage site in these tRNAs (Krzyzosiak et al., 1988; Ciesiolka et al., 1989). The exact identity of base pairs comprising the stems is probably not a critical constraint for the reaction, since the five tRNAs that demonstrate strong cleavage at p18 do not possess significant homology in these regions (Ciesolka et al., 1989). One important component of the motif is the interaction between T- and D-loops, and the binding of metal ions to the variable pocket formed by their association. Although there is a high degree of sequence invariance among all tRNAs in this region, only a few retain the ability to be cleaved by lead site specifically. The motif does not seem to require a strict set of nucleotides in the D-loop, although the identity of the base on the 3′ side of the cleavage site is always G in cases so far described. The T-loop residues, all except for those at position 59, are either invariant or semi-invariant in all tRNAs. The reaction in unmodified transcripts of tRNA^{Phe} is sensitive not only to mutations that disrupt the interaction between T- and D-loops but also to mutations that rupture the base of the T-loop, or the U_{54}–A_{58} intraloop base pair (Behlen et al., 1990). The dinucleotide sequence U_{59}–C_{60} was formerly thought to be critical for the binding and positioning of lead ion (Krzyzosiak et al., 1988). Examination of lead cleavage in other tRNAs has shown that the elongator tRNA^{Met} from both yeast (A_{59}–C_{60}) and lupin (G_{59}–C_{60}) are cleaved at p18, suggesting that only C_{60} needs to be conserved and that A, G, and U are acceptable at position 59 (Ciesolka et al., 1989). It is interesting that the required C_{60} is a semi-invariant, whereas 59 is a variable base. The high degree of base conservation in the T- and D-loops may be related to the maintenance of a flexible ligand sphere for metal ion binding in the pocket formed by their association. The functional role of such a feature as it relates to the current structural and functional roles of tRNA is unclear, but this feature may represent the vestige of an earlier, possibly catalytic role for the highly conserved core found within many tRNAs.

The catalytic RNA cleavage reactions based on the yeast tRNA^{Phe} and the specific autocleavage of other tRNAs have no apparent biological significance; however, they suggest that there may exist folding motifs for other RNAs that can utilize metal ions to perform site-specific cleavages. Computer searches have identified the existence of several possible tRNA-like arrangements in non-tRNA sequences, although the ability of these to participate in metal-catalyzed hydrolytic reactions remains to be determined (Pan et al., 1991). These results reenforce the notion that specific metal ion induced cleavages of tRNA may reflect a general property of RNA which has evolved into the highly specific self-cleaving RNA processing events. The eventual appearance of such motifs in intron sequences would have selective advantages.

A lack of knowledge of the tertiary interactions present in the hammerhead catalytic RNA motif makes it difficult to determine how the two cleavage motifs are related. Our work demonstrates for the first time that a complex derived from yeast tRNA^{Phe} consisting of three helices (1–24/46–76) can undergo catalytic reaction. The helical arrangement is shared by the hammerhead reaction core. The identical nature of the cleavage end products [2′,3′-cyclic phosphate; Brown et al. (1985)] and the similarity in turnover rates and energies

of activation make it appear likely that the tRNA fragment reactions are mechanistically related to the hammerhead case. Factors which influence the cleavage rates of the catalytic RNA reactions derived from the yeast $tRNA^{Phe}$ may also be important in modifying the cleavage rates of hammerhead ribozymes.

All tRNAs so far examined that show lead cleavage at p18 also demonstrate cleavage with magnesium and lanthanide ions. In these cases, the strong cleavage site is shifted to p16 (Krzyzosiak et al., 1988; Marciniec et al., 1989; Wintermeyer & Zachau, 1973). These reactions are usually less selective than those obtained with Pb^{2+}. An interesting exception to this is the lupin initiator $tRNA^{Met}$, which is cleaved with greater specificity in the presence of Mg^{2+} (Ciesiolka et al., 1989). This implies that tRNA-based catalytic RNA reactions may be possible using biologically ubiquitous ions rather than toxic, nonessential ones such as lead.

REFERENCES

Altman, S. (1989) *Adv. Enzymol. 62*, 1–36.

Arendes, J., Carl, P. L., & Sugino, A. (1982) *J. Biol. Chem. 257*, 4719–4722.

Behlen, L. S., Sampson, J. R., DiRenzo, A. B., & Uhlenbeck, O. C. (1990) *Biochemistry 29*, 2515–2523.

Borer, P. N. (1976) in *CRC Handbook of Chemistry and Molecular Biology. Nucleic Acids Vol. I*, 3rd ed. (Fassman, G. D., Ed.) p 589, CRC Press, Boca Raton, Fl.

Boyle, J., Robilland, G. T., & Kim, S. H. (1980) *J. Mol. Biol. 139*, 601–625.

Boyle, J. A., Kim, S. H., & Cole, P. E. (1983) *Biochemistry 22*, 741–744.

Brown, R. S., Hingerty, B. E., Dewan, J. C., & Klug, A. (1983) *Nature 303*, 543–546.

Brown, R. S., Dewan, J. C., & Klug, A. (1985) *Biochemistry 24*, 4785–4801.

Butzow, J. J., & Eichorn, G. L. (1965) *Biopolymers 3*, 95–107.

Butzow, J. J., & Eichorn, G. L. (1971) *Biochemistry 10*, 2019–2027.

Cameron, V., & Uhlenbeck, O. (1973) *Biochem. Biophys. Res. Commun. 50*, 635–640.

Cech, T. R. (1987) *Science 236*, 1532–1539.

Ciesiolka, J., Wrzesinski, J., Gornicki, P., Podkowinski, J., & Krzyzosiak, W. J. (1989) *Eur. J. Biochem. 186*, 71–77.

Cubellis, M. V., Marino, G., Mayol, L., Piccialli, G., & Sannia, G. (1985) *J. Chromatogr. 329*, 406–414.

Dahm, S. C., & Uhlenbeck, O. C. (1991) *Biochemistry 30*, 9464–9469.

Davanloo, P., Sprinzl, M., & Cramer, F. (1979) *Biochemistry 18*, 3189–3199.

Dimroth, K., & Witzel, H. (1959) *Ann. Chem. 620*, 109–122.

Dixon, M., & Webb, E. (1979) *The Enzymes*, pp 164–182, Academic Press, New York.

Donis-Keller, H. (1979) *Nucleic Acids Res. 7*, 179–193.

Eisenthal, R., & Cornish-Bowden, A. (1974) *Biochem. J. 139*, 715–720.

Farkas, W. R. (1968) *Biochem. Biophys. Acta 155*, 401–409.

Guerrier-Takada, G., Haydock, K., Allen, L., & Altman, S. (1986) *Biochemistry 25*, 1509–1515.

Hall, K. B., Sampson, J. R., Uhlenbeck, O. C., & Redfield, A. G. (1989) *Biochemistry 28*, 5794–5801.

Inoue, H., Hayase, Y., Iwai, S., & Ohtsuka, E. (1987) *FEBS Lett. 215*, 327–330.

Jack, A., Ladner, J. E., Rhodes, D., Brown, R. S., & Klug, A. (1977) *J. Mol. Biol. 111*, 315–328.

Johnston, P. D., & Redfield, A. G. (1979) in *Transfer RNA: Structure, Properties and Recognition* (Abelson, J., Schimmel, P. R., Soll, D., Eds.) p 191, Cold Spring Harbor Laboratory, Cold Spring Harbor, NY.

Katayanagi, K., Miyagawa, M., Matsushima, M., Ishikawa, M., Kanaya, S., Ikehana, M., Matsuzaki, T., & Morikawa, K. (1990) *Nature 347*, 306–309.

Keller, W., & Crouch, R. (1972) *Proc. Natl. Acad. Sci. U.S.A. 69*, 3360–3364.

Kim, S. H., & Sussman, J. L. (1976) *Nature 260*, 645–646.

Kim, S. H., Suddath, F. L., Quigley, G. J., McPherson, A., Sussman, J. L., Wang, A. H. J., Seeman, N. C., & Rich, A. (1974) *Science 185*, 435–439.

Kistiakowsky, G. B., & Lumry, R. (1949) *J. Am. Chem. Soc. 71*, 2006–2013.

Krzyzosiak, W. J., Marciniec, T., Wiewiorowski, M., Romby, P., Ebel, J. P., & Giege, R. (1988) *Biochemistry 27*, 5771–5777.

Lorenz, S., Hartmann, R. K., Piel, N., Ulbrich, N., & Erdmann, V. A. (1987) *Eur. J. Biochem. 163*, 239–246.

Massey, V. (1953) *Biochem. J. 53*, 72–79.

Marciniec, T., Ciesiolka, J., Wrzesinski, J., & Krzyzosiak, W. J. (1989) *FEBS Lett. 243*, 293–298.

Minton, A. P. (1981) *Biopolymers 20*, 2093–2120.

Minton, A. P. (1983) *Mol. Cell. Biochem. 55*, 119–140.

Pan, T., Gutell, R. R., & Uhlenbeck, O. C. (1991) *Science 254*, 1361–1364.

Prinz, H., Maeliecke, A., & Cramer, F. (1974) *Biochemistry 13*, 1322–1326.

Quigley, G. J., Teeter, M. M., & Rich, A. (1978) *Proc. Natl. Acad. Sci. U.S.A. 75*, 64–68.

Reid, B. R. (1981) *Annu. Rev. Biochem. 50*, 969–996.

Reisner, D., Maass, G., Thiebe, R., Philippsen, P., Zachau, H. G. (1973) *Eur. J. Biochem. 36*, 76–88.

Robertus, J. D., Ladner, J. E., Finch, J. T., Rhodes, D., Brown, S. R., Clark, B. F. C., & Klug, A. (1974) *Nature 250*, 546–551.

Sampson, J. R., Sullivan, F. X., Behlen, L. S., DiRenzo, A. B., & Uhlenbeck, O. C. (1987) *Cold Spring Harbor Symp. Quant. Biol. 52*, 267–275.

Simsek, M., Petrissant, G., & RajBhandary, U. L. (1973) *Proc. Natl. Acad. Sci. U.S.A. 70*, 2600–2604.

Steely, H. T., Jr., Gray, D. M., Lang, D., & Maestre, M. F. (1986) *Biopolymers 25*, 91–117.

Stepanova, O. B., Metelev, V. G., Chichkova, N. V., Smirnov, V. D., Rodionova, N. P., Atabekov, J. G., Boydanov, A. A., & Shabarova, Z. A. (1979) *FEBS Lett. 103*, 197–199.

Thiebe, R., & Zachau, H. G. (1971) *Methods Enzymol. 20*, 179–182.

Uhlenbeck, O. C. (1987) *Nature 328*, 596–600.

Werner, C., Krebs, B., Keith, G., & Dirheimer, G. (1976) *Biochim. Biophys. Acta 432*, 161–175.

Wintermeyer, W., & Zachau, H. G. (1970) *FEBS Lett. 11*, 160–164.

Wintermeyer, W., & Zachau, H. G. (1973) *Biochim. Biophys. Acta 299*, 82–90.

Yang, W., Hendrickson, W. A., Crouch, R. J., & Satow, Y. (1990) *Science 249*, 1398–1405.